Microphase separation in multiblock copolymer melts: Nonconventional morphologies and two-length-scale switching

Yuliya G Smirnova
Laboratory of Polymer Chemistry and Materials Science Centre, University of Groningen, Nijenborgh 4, 9747 AG Groningen, The Netherlands and Moscow State University, Moscow 119899, Russia

Gerrit ten Brinke[a)]
Laboratory of Polymer Chemistry and Materials Science Centre, University of Groningen, Nijenborgh 4, 9747 AG Groningen, The Netherlands

Igor Ya. Erukhimovich[b)]
Moscow State University, Moscow 119899, Russia

(Received 17 June 2005; accepted 28 November 2005; published online 3 February 2006)

The phase behavior of $A_{fmN}(B_{N/2}A_{N/2})B_{(1-f)mN}$ multiblock copolymer melts is studied within the weak segregation theory. The interplay between ordering on different length scales is shown to cause dramatic changes both in the ordered phase symmetry and periodicity upon small variation of the architectural parameters of the macromolecules. Phase diagrams are presented in the $(f,\chi N)$ plane (χ is the Flory-Huggins parameter) for various values of the architecture parameters n and m. Near the critical surface, i.e., for $(f-0.5)^2 \ll 1$, such nonconventional cubic phases as the face-centered cubic (FCC), simple cubic (SC), (double) gyroid, and the so-called BCC_2 (single gyroid) are found to be stable. The lamellar morphology is shown to be replaced by BCC_2, FCC, or SC (depending on the structural parameters) as the most stable low-temperature phase.
 [DOI: 10.1063/1.2161200]

I. INTRODUCTION

Many block copolymer melts undergo the so-called order-disorder transitions (ODTs) resulting in the formation of ordered morphologies with the symmetry of a crystal lattice.[1–4] The physical reason for this ordering, also called "microphase separation," is the competition between the short-range segregation and long-range stabilization tendencies. Indeed, with a decrease of the temperature the energy gain upon local segregation grows as compared to the entropic loss accompanying such a segregation, while large-scale demixing is forbidden due to covalent bonding of the different blocks. As a result, below a certain (spinodal) temperature the disordered state becomes unstable with respect to the growth of the amplitudes A of those local concentration fluctuations described by an order parameter, $\Psi(\boldsymbol{r}) = A\cos(\boldsymbol{qr})$, whose wave numbers q are close to a certain critical value $q^* \neq 0$.[1,5,6] By varying the system parameters different morphologies may appear at the order-disorder and order-order phase transitions,[7] and the aim of the theory is to determine the symmetry and geometry of the most stable ordered phases for a copolymer given its architecture and temperature.

In a more general context, the theory of microphase separation in block copolymer systems provides a unique opportunity to test the general phenomenological concepts of the statistical theory of solid-liquid transition via a rigorous microscopic consideration. Indeed, the universal (Gaussian) conformational behavior of the long polymer blocks makes it possible to develop microscopic theory of microphase separation in block copolymer melts, which was first done by Leibler[1] for diblock copolymers.

Using the mean-field approximation Leibler[1] found that the thermodynamically stable ordered morphologies for diblock copolymers A_nB_m are the body-centered cubic lattice (BCC) and the hexagonal (HEX) and lamellar (LAM) structures. All the first-order phase-transition lines between these ordered phases and between the BCC and disordered phase (DIS) merge at a critical point in the $(\tilde{\chi},f)$ plane (as usual, here $f=n/N$ is the composition of the A monomers, $N=n+m$ is the total degree of polymerization of the diblock copolymer, and $\tilde{\chi}=N\chi$, where χ is the Flory-Huggins interaction parameter). If the statistical segment lengths and excluded volumes are the same for all the monomer species, which is assumed hereafter for simplicity, then the critical point is located at $f=0.5$, which corresponds to the symmetric diblock copolymer melt. The order-disorder transition at this point is the second-order phase transition into the lamellar phase.[1]

The Leibler theory[1] has been generalized by Fredrickson and Helfand[8] with due regard for fluctuation corrections and by other authors to melts of block copolymers with some more complicated architectures[9,10] (see also Refs. 2–4 and references therein). It is referred to as the weak segregation theory (WST) and is the first (and, up to our knowledge, the only) microscopic consideration implementing the Landau

[a)]Electronic mail: g.ten.brinke@rug.nl
[b)]Electronic mail: ierukhs@polly.phys.msu.ru

idea of the second-order solid-liquid transition.[11] (The latter is also referred to as the weak crystallization theory.[12–14])

Unfortunately, the region of the WST applicability corresponds to a rather narrow vicinity of the critical point. Besides, the WST employs the so-called first harmonics approximation and it is often believed that within this approximation "the predictions about ordered structures are limited to classical phases of lamellar, hexagonal, and body-centered cubic structures, and consequently the possibility of other structures such as bicontinuous structures, e.g., double gyroid, is excluded. To overcome this limitation the so-called harmonic correction is used by including the higher harmonics."[15] So, during the last decade the so-called self-consistent field theory (SCFT) by Matsen and co-workers[16,17] which is free of these shortcomings, became dominant in understanding the behavior of the ordering block copolymer systems. In contrast to the WST, the SCFT has a much broader region of applicability, which enabled Matsen and Schick[16] to explain the stability of the gyroid (G) phase just observed experimentally[18,19] at some distance from the critical point.

The application of the WST requires calculation of cumbersome expressions for the so-called higher structural correlators; still, the SCFT is no less technically involved and much more time consuming (in terms of numerical calculations) than the WST. Besides, unlike the SCFT, a considerable part of the calculations necessary to build the phase diagrams within the WST can be done analytically. Most importantly, however, a general WS analysis[20,21] has demonstrated that, contrary to the aforementioned belief, under certain conditions the most stable phases around the critical point are not necessarily the classic ones. Instead, some others cubic phases such as double gyroid (G), simple cubic (SC), face-centered cubic (FCC), and the so-called BCC_2 (Ref. 20) (we refer to all the phases but BCC, HEX, and LAM as the nonconventional ones) may be stable, whereas the classic phases are metastable only. The conditions for the nonconventional phases to be stable even within the first harmonics approximation have been found.[21] (These conditions ensure that the phase-transition lines G-HEX, on the one side, and G-LAM (or G-BCC_2, G-FCC, G-SC) on the other side extend, unlike the situation in diblock copolymers, up to the very critical point.)

In general, the best strategy to build theoretically phase diagrams of block copolymers is to base the SCFT analysis in a broad range of the system parameters on the results of the WST analysis close to the critical point(s), where both theories are expected to provide identical results. Consistent with this strategy, in this paper we apply the WST to a new class of copolymer systems. We report a new type of phase behavior: an abrupt and tremendous increase of the period of the supercrystal morphologies as well as the occurrence of nonconventional morphologies with a gradual change of the architecture for some specially designed binary block copolymers.

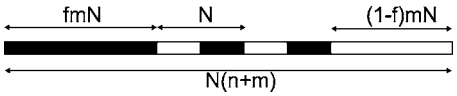

FIG. 1. The architecture of the macromolecules considered.

This prediction is based on two recent observations, the first of which is the discovery of so-called two-length-scale behavior. To our knowledge, it was first described by Holyst and Schick[22] who considered a symmetric ternary mixture of A and B homopolymers and AB block copolymers. They found that there is a line, which they called equimaxima line, where the homopolymer A - homopolymer B correlation function reveals two peaks of the same height, one of which is always located at $q=0$ and the other one at certain $q^* \neq 0$. However, this equimaxima line was found to be located entirely within the stability region of the disordered phase, one of the peaks being eliminated when approaching the spinodal. We refer to such a behavior as a *virtual* two-length-scale one. The *real* two-length-scale behavior has been first discovered by Nap and co-workers[23,24] who found that melts of some specially designed multiblock and comb-coil macromolecules, whose architecture is characterized by two intrinsic lengths, may become unstable *simultaneously* with respect to critical fluctuations with two rather different characteristic wave numbers q_1^* and q_2^*. (It is worth noting, that real two-length-scale behavior has been found also in blends of ABC and AC block copolymers[25,26] and solutions of multiblock copolymers.[27]) The phase diagrams obtained by Nap and co-workers[24,28] within both the WST and SCFT demonstrated that such a two-length-scale instability results in order-order transitions between lattices with different periods.

The second observation that is relevant to our paper is the finding[25,29,30] that, due to symmetry, the WS theory is applicable to the symmetric ternary $A_{fN}B_{(1-2f)N}C_{fN}$ triblock copolymers with an arbitrary value of f if the middle block is nonselective with respect to the end blocks. Here nonconventional phases BCC_2, FCC, and SC appear with increasing middle block composition $f_B=1-2f$.

In the present work we consider monodispersed melts of AB multiblock copolymers, whose architecture is shown in Fig. 1. The multiblock copolymer is built of a middle part consisting of n diblock units ($A_{N/2}B_{N/2}$) of size N. The homopolymers A_{fmN} and $B_{(1-f)mN}$ ($0 \leqslant f \leqslant 1$) are attached at the respective ends of the multiblock. Hence, the parameter m characterizes the relative total length of the tails with respect to that of the diblock unit, while the parameter f characterizes the asymmetry ratio of the end blocks. For $f=0.5$ the system has equal amounts of A and B monomers and is perfectly symmetric. The most asymmetric case corresponds to $f=0$ (or $f=1$), when the macromolecules contain only one homopolymer block B (or A). The total degree of polymerization reads $N_{\mathrm{tot}}=nN+Nmf+Nm(1-f)=N(n+m)$.

Experimentally, there is always a distribution of the described multiblock copolymer macromolecules over the lengths and number of the blocks since the real macromolecules are obtained via an intrinsically statistical polymerization process. Accordingly, both ordering (microphase separa-

tion) and macrophase separation can occur. In the latter case coexistence of phases with different crystal symmetry or between ordered and disordered (homogeneous) phases may take place. However, the region of such a coexistence occupies a rather narrow region on the corresponding phase diagrams[31,32] if only the molecular structure distribution is not too broad. Therefore, in this paper we disregard the effect of the structural polydispersity (and, thus, the effects of the phase coexistence) and focus only on the architecture-caused peculiarities of the phase diagrams. Of course, this is fully validated if the system is monodispersed, i.e., consists of identical macromolecules however complicated their structure.

If $m=0$ or $m=1$ with $f=0.5$, then the system is just a melt of symmetric multiblock copolymers consisting of n or $n+1$ diblock units ($A_{N/2}B_{N/2}$), respectively. In this case, on reducing the temperature, lamellar A and B domains are formed. Both within the random-phase approximation (RPA),[33–35] WST,[10] and SCFT[36] the phase behavior of regular multiblock copolymers is shown to be qualitatively similar to that of diblock copolymer melts. However, the situation changes drastically for larger m. In this case with a temperature decrease the long tail blocks are expected first to segregate into separate A and B domains whereas the shorter blocks of the alternating middle block are still mixed. We show below that these expectations are fully justified and that the corresponding critical parameter surfaces do exist and in their vicinity the phase diagrams can be quantitatively built within the WST. For m large, on a further reduction of the temperature the shorter blocks will also start to phase separate. This is, however, beyond the scope of the present WST analysis.

The architecture of the polymer of interest does resemble the structure of the ACB triblock, the middle part $(A_{N/2}B_{N/2})_n$ corresponding to the nonselective block C. We expect that, at least for $f=0.5$, the WST is applicable and the above mentioned complicated cubic structures can be stable. At the same time the middle part $(A_{N/2}B_{N/2})_n$ has its own intrinsic characteristic length, which may, in turn, dictate another period of microphase separation. Hence, this polymer has two different length scales, one related to the size of the diblock N and another to the total size of the macromolecules. Therefore, we expect rather complicated phase behavior of these melts, which we study here using the weak segregation theory.

The rest of the paper is organized as follows. In Sec. II the theory used is briefly outlined. In Sec. III the results are discussed.

II. THEORY

To describe microphase separation it is convenient to introduce the order parameter $\Psi_i(\mathbf{r})=\phi_i(\mathbf{r})-f_i$, which is the deviation of the volume fraction $\phi_i(\mathbf{r})$ of monomers of the ith sort ($i=A,B$) at point $\mathbf{r}$ from its average value f_i. We assume the melt to be incompressible. Hence, $\Psi_A(\mathbf{r})=-\Psi_B(\mathbf{r})$, and in what follows the simplified notation $\Psi_A(\mathbf{r})\equiv\Psi(\mathbf{r})$ is used.

Given a distribution $\phi_i(\mathbf{r})$, the free energy F of a binary incompressible system is conventionally assumed to be the sum

$$F=F_{\mathrm{str}}\{\phi_i(\mathbf{r})\}+\chi\int\phi_A(\mathbf{r})\phi_B(\mathbf{r})\mathrm{d}\mathbf{r}, \tag{1}$$

where the first contribution is related to the entropy of the inhomogeneous distribution of the Gaussian macromolecules characterized by the order parameter $\Psi(\mathbf{r})$ and the second (monomer-monomer interaction) part of the free energy is accounted for via a specified value of the χ parameter ($\chi>0$) within the Flory-Huggins lattice approach.[37]

In Fourier space the order parameter $\Psi(\mathbf{q})=\int\Psi(\mathbf{r})e^{i\mathbf{q}\mathbf{r}}\mathrm{d}\mathbf{r}$ is the amplitude of the harmonic concentration wave with the wave vector $\mathbf{q}$ and a finite period $L=2\pi/|\mathbf{q}|$. In the vicinity of the critical point the order parameter is sufficiently small and the free energy may be expanded in terms of the order parameter. The fourth-order Landau expansion reads[1]

$$\frac{\Delta F}{k_BT}=\sum_{n=2}^{n=4}\frac{1}{n!\,(2\pi)^{3n}}\int\Gamma_n(\mathbf{q}_1,\ldots,\mathbf{q}_n)\,\delta(\mathbf{q}_1+\cdots+\mathbf{q}_n)\times\prod_{i=1}^{i=n}\Psi(\mathbf{q}_i)\mathrm{d}\mathbf{q}_i. \tag{2}$$

Here the nth-order vertex functions Γ_n are related to the nth-order Gaussian single-chain correlation functions $g_{\alpha_1\ldots\alpha_n}(\mathbf{r}_1\ldots\mathbf{r}_n)$ as first shown by Leibler.[1] The explicit expressions for these correlators are rather cumbersome even in the simplest case of diblock copolymers. For more complicated architectures (asymmetric triblock and trigraft, polyblock and polygraft, and star copolymers) the list of the correlators occupies 24 pages of the supplementary material available for Ref. 10. In particular, the second-order vertex function $\Gamma_2(\mathbf{q}_1,\mathbf{q}_2)$ reads

$$\Gamma_2(\mathbf{q}_1,\mathbf{q}_2)=V\delta(\mathbf{q}_1+\mathbf{q}_2)\,\gamma_2(q_1)=V(\tilde{g}^{-1}(q_1)-2\chi), \tag{3}$$

where

$$\tilde{g}(q)=\frac{g_{AA}(q)q_{BB}(q)-g_{AB}^2(q)}{g_{AA}(q)+2g_{AB}(q)+g_{BB}(q)} \tag{4}$$

and the functions $g_{AA}(q)$, $g_{BB}(q)$, and $g_{AB}(q)$ for our system are defined in the Appendix.

For polydisperse systems one more, the so-called nonlocal fourth-order term, which implicitly describes the effects of macromolecules redistribution between the coexisting phases, should be included into the Landau expansion (2). The nonlocal term was first calculated for long random AB copolymer chains by Shakhnovich and Gutin.[38] For arbitrary molecular structural distributions it was found by Panyukov and Kuchanov,[39] Fredrickson *et al.*,[40] and Erukhimovich and Dobrynin.[31] The phase diagrams of such polydisperse systems with due regard for the nonlocal term were calculated in Refs. 31, 32, 41, and 42. For monodispersed systems, where, obviously, no macrophase separation can occur, the nonlocal term is identically zero.[31,39,40]

For fixed structural parameters (n,m,f) the function Γ_2 determines the spinodal surface, which bounds the region in the space (χ,n,m,f), where the disordered state of the system becomes unstable with respect to the growth of the concentration fluctuations of a certain critical wave length $L=2\pi/q^*$,[1,5,6]

$$\min \Gamma_2(q) = \Gamma_2(q^*) = 0. \tag{5}$$

It follows from the spinodal equation (5) that the spinodal value of χ parameter reads

$$\chi_s = \tilde{g}^{-1}(q^*)/2, \tag{6}$$

where q^* is the location of the minimum of the function $\Gamma_2(q)$ [or $\tilde{g}^{-1}(q)$].

For $\chi > \chi_s$ an ordered structure with period $L=2\pi/q^*$ appears. Therefore, the order parameter acquires the symmetry of a crystal lattice with this period and can be expanded in a Fourier series

$$\Psi(\boldsymbol{r}) = \sum_{\boldsymbol{q}_i} A(\boldsymbol{q}_i)\exp i(\boldsymbol{q}_i\boldsymbol{r} + \varphi(\boldsymbol{q}_i)), \tag{7}$$

where $\boldsymbol{q}_i$ is the set of vectors, which belong to the reciprocal lattice corresponding to the ordered structure of interest. The phases $\varphi(\boldsymbol{q}_i)$ are defined by the symmetry group of the lattice. In the weak segregation regime one adopts usually the first harmonics approximation, which corresponds to taking into account in the series (7) only $2k$ vectors belonging to the first coordination sphere of the length q^*. Due to the symmetry all amplitudes of the first harmonic are the same, and it is convenient to normalize the amplitudes via the relationship $A(\boldsymbol{q}_i) \equiv A/\sqrt{k}$. Substituting (7) into (2) we obtain for the free energy,

$$\Delta F/T = \tau A^2 + \alpha A^3 + \beta A^4. \tag{8}$$

Here the temperature is measured in the energetic units, in which the Boltzmann constant is unity ($k_B=1$), and the following designations are introduced:

$$\tau = \Gamma_2(q^*), \tag{9}$$

$$\alpha_k = \frac{\gamma}{k^{3/2}} \sum_3 \cos \Omega_j^{(3)} \tag{10}$$

and

$$\beta_k = \frac{\lambda_0(0)}{4k} + \frac{\sum \lambda_0(h) + \sum_4 \lambda(h_1,h_2,h_3)\cos \Omega_j^{(4)}}{k^2}. \tag{11}$$

In Eqs. (9)–(11) we used the Leibler designations and parameters[1]

$$h_1 = [(\boldsymbol{q}_1 + \boldsymbol{q}_2)/q^*]^2,$$
$$h_2 = [(\boldsymbol{q}_1 + \boldsymbol{q}_3)/q^*]^2, \quad h_3 = [(\boldsymbol{q}_1 + \boldsymbol{q}_4)/q^*]^2, \tag{12}$$

$$\gamma = \Gamma_3(\boldsymbol{q}_1,\boldsymbol{q}_2,\boldsymbol{q}_3), \tag{13}$$

and

$$\lambda_0(h) = \lambda(0,h,4-h), \quad \lambda(h_1,h_2,h_3) = \Gamma_4(\boldsymbol{q}_1,\boldsymbol{q}_2,\boldsymbol{q}_3,\boldsymbol{q}_4), \tag{14}$$

with $|\boldsymbol{q}_i| = q^*$ and $\Sigma \boldsymbol{q}_i = 0$. The phases $\Omega_j^{(n)}$ are the algebraic sums of the phases $\varphi(\boldsymbol{q}_i)$ for the triplets and noncoplanar quartets of the vectors involved in the definition of corresponding γ and λ, the symbol Σ_n designates summation over all sets of such n vectors. The first summation in Eq. (11) is over all pairs of noncollinear vectors $\boldsymbol{q}_i$ and $\boldsymbol{q}_j$.

Finally, we minimize the free energy (8) with respect to the amplitude A (the resulting amplitude is required to be small enough to ensure validity of the WST) and compare the free-energy values for different lattices to determine the most stable phase. For those phases, whose stability is studied in this paper, the explicit expressions for the coefficients α and β are listed below.

First, the well-known expressions for the classic LAM, HEX, and BCC phases read[1]

$$\alpha_{\mathrm{LAM}} = 0, \quad \beta_{\mathrm{LAM}} = \lambda_0(0)/4, \tag{15}$$

$$\alpha_{\mathrm{HEX}} = 2\gamma/3^{3/2}, \quad \beta_{\mathrm{HEX}} = [\lambda_0(0) + 4\lambda_0(1)]/12, \tag{16}$$

$$\alpha_{\mathrm{BCC}} = 8\gamma/6^{3/2},$$
$$\beta_{\mathrm{BCC}} = [\lambda_0(0) + 8\lambda_0(1) + 2\lambda_0(2) + 4\lambda(1,2)]/24. \tag{17}$$

We also take into account a nonconventional phase, which surprisingly appears to be stable in the weakly segregated multiblock copolymers $A_{fmN}(B_{N/2}A_{N/2})_nB_{(1-f)mN}$ within an interval of the relative tail length m. This phase was first introduced by Brazovskii *et al.*[20] and is closely related to the BCC phase, which was the reason to refer to it as the BCC_2 phase. Indeed, the BCC_2 is formed if one keeps in the order parameter (7) the same six vectors (and the opposite ones) of the first harmonic,

$$\boldsymbol{q}_1 = \frac{q^*}{\sqrt{2}}(0,1-1), \quad \boldsymbol{q}_2 = \frac{q^*}{\sqrt{2}}(-1,0,1),$$
$$\boldsymbol{q}_3 = \frac{q^*}{\sqrt{2}}(1,-1,0),$$
$$\boldsymbol{q}_4 = \frac{q^*}{\sqrt{2}}(0,-1-1), \quad \boldsymbol{q}_5 = \frac{q^*}{\sqrt{2}}(-1,0,-1), \tag{18}$$
$$\boldsymbol{q}_6 = \frac{q^*}{\sqrt{2}}(-1,-1,0),$$

which are known to correspond to the conventional BCC morphology if all the phase shifts $\varphi(\boldsymbol{q}_i)$ appearing in the trial function (7) are zero. However, the phase shifts necessary to form the BCC_2 lattice[20] are different,

$$\varphi_1 = \varphi_2 = \varphi_3 = \pi/2, \quad \varphi_4 = \varphi_5 = \varphi_6 = 0. \tag{19}$$

As consistent with the definitions [(18) and (19)], the order parameter (7) for BCC_2 reads

$$\Psi(\boldsymbol{r}) = 2A/(\sqrt{6})[\cos(\tilde{x}+\tilde{y}) + \cos(\tilde{y}+\tilde{z}) + \cos(\tilde{z}+\tilde{x}) - \sin(\tilde{x}-\tilde{y}) - \sin(\tilde{y}-\tilde{z}) - \sin(\tilde{z}-\tilde{x})], \quad (20)$$

where the waved coordinates are scaled as compared to the original ones according to the rule $\tilde{s}=sq^*/\sqrt{2}$. The fact that the series (20) contains both cosines and sines implies[43] that the BCC_2 morphology is noncentrosymmetric. Thus, it seems to be the simplest (and the only one up to now) cubic noncentrosymmetric morphology that can be described (and for some cases predicted as shown below) within the WS theory.

The shift $\tilde{x}=X+\pi/4$, $\tilde{y}=Y+\pi/4$, and $\tilde{z}=Z+\pi/4$ of the origin of the coordinate system reduces the order-parameter profile (20) to the form

$$\Psi(\boldsymbol{r}) = \tilde{A}[\sin X \cos Y + \sin Z \cos X + \sin Y \cos Z]. \quad (21)$$

The level surfaces of the order parameter (21), i.e., the surfaces satisfying the condition

$$\sin X \cos Y + \sin Z \cos X + \sin Y \cos Z = C, \quad (22)$$

are known[44] to be representatives of the triple periodic bicontinuous surfaces having the symmetry $I4_132$ of the space group number 214. In particular, the surface (22) with $C=0$ is well known[44] as the gyroid surface because it appears rather similar to the Schoen's gyroid minimal surface. We also refer to the BCC_2 lattice as the single gyroid (SG) in contrast to the popular nonconventional cubic lattice having the symmetry $Ia\bar{3}d$ of the space group number 230, which is also called gyroid or double gyroid (G). For the two gyroid phases the coefficients α and β read[20,21,45]

$$\alpha_{BCC_2} = 0, \qquad \beta_{BCC_2} = [\lambda_0(0) + 8\lambda_0(1) + 2\lambda_0(2) - 4\lambda(1,2)]/24, \quad (23)$$

$$\alpha_G = \gamma/3^{3/2}, \quad \beta_G = [\Lambda_1 - 2\Lambda_2 - 4\lambda(1/3,2/3)]/48, \quad (24)$$

where the designations $\Lambda_1=\lambda_0(0)+2[\lambda_0(4/3)+2[\lambda_0(1/3)+\lambda_0(2/3)+\lambda_0(1)+2\lambda_0(5/3)]]$ and $\Lambda_2=2\lambda(2/3,5/3)-\lambda(2/3,2/3)$ are introduced. Finally, for the FCC, simple square (SQ), and SC phases, which we also include in the list of the competing phases, the coefficients α and β read[1]

$$\alpha_{SQ} = 0, \quad \beta_{SQ} = [\lambda_0(0) + 2\lambda_0(2)]/8, \quad (25)$$

$$\alpha_{SC} = 0, \quad \beta_{SC} = [\lambda_0(0) + 4\lambda_0(2)]/12, \quad (26)$$

$$\alpha_{FCC} = 0, \quad \beta_{FCC} = [\lambda_0(0) + 6\lambda_0(4/3) - 2\lambda(4/3,4/3)]/16. \quad (27)$$

There exists a so-called critical surface in the space (f,n,m),

$$\Gamma_3(\boldsymbol{q}_1,\boldsymbol{q}_2,\boldsymbol{q}_3,f,n,m) = 0 \quad (|\boldsymbol{q}_i| = q^*,\ \boldsymbol{q}_1+\boldsymbol{q}_2+\boldsymbol{q}_3 = 0), \quad (28)$$

where the coefficient α in the free energy (8) equals zero. At any critical point (set of parameters, which belongs both to the critical surface and spinodal) the phase transition is continuous and, therefore, starts with zero-order parameter. Thus, the WS theory is expected to be valid in the vicinity of the critical points.

For simple block copolymer systems such as diblock,[1] triblock and trigraft,[9,10] multiblock and multigraft (comblike), as well as various star[10] copolymers the WST predicts that only the lamellar, hexagonal, and body-centered cubic structures are stable, which is due to fact that for these systems the fourth-order vertices can be well approximated[8] as

$$\Gamma_4(\boldsymbol{q}_1,\boldsymbol{q}_2,\boldsymbol{q}_3,\boldsymbol{q}_4) = \Gamma_4(q_1,q_2,q_3,q_4). \quad (29)$$

However, one can check straightforwardly that for the two-length-scale multiblock copolymers under consideration the approximation (29) is not valid since the values of the fourth-order structural correlators strongly depend on the angles between the vectors $\boldsymbol{q}_i$ as well. It is the consequence of this strong angle dependence that some other more complicated structures (which are only metastable for simple diblock copolymers) become stable. The phase diagrams obtained are presented in the next section.

III. RESULTS AND DISCUSSION

A. Symmetric systems ($f=0.5$)

The scattering behavior of $A_{fmN}(B_{N/2}A_{N/2})_nB_{(1-f)mN}$ block copolymers is rather different from that of the simple copolymer melts (e.g., diblock copolymer $A_{fN}B_{(1-f)N}$, which is the particular case of the architecture $A_{fmN}(B_{N/2}A_{N/2})_nB_{(1-f)mN}$ with $n=0$, $m=1$). For the latter only one maximum is observed in the structure factor $S(q) \sim (\Gamma_2(q))^{-1}$ and, accordingly, the function $\Gamma_2(q)$, which determines the spinodal, has only one minimum. In contrast, for the multiblock copolymers of interest there is a region in the (n,m) plane called the bifurcation region, where the structure factor exhibits *two* maxima. The presence of a maximum of $S(q)$ [i.e., a minimum of $\Gamma_2(q)$ at $q=q^*$] indicates the existence of a characteristic length scale $L=2\pi/q^*$ of the weekly modulated ordered morphology occurring in the weak segregation regime. The presence of two maxima indicates that two different length scales may arise.[23,24,26] One of these scales is determined by the radius of gyration of the basic diblock unit AB of the multiblock middle part of the molecule, and the other one by the radius of gyration of the macromolecule as a whole.

The so-called classification diagram[23] delineating the bifurcation region for the symmetric systems $A_{mN/2}(B_{N/2}A_{N/2})_nB_{mN/2}$ is shown in Fig. 2(a). Even though n is an integer, by definition, for convenience we treat it as a continuous variable and plot, accordingly, continuous lines in the classification and phase diagrams. The border lines of the bifurcation region merge at the point ($n=5.17$ and $m=2.18$) called the bifurcation point.[23,24] The equimaxima line where both maxima of the structure factor diverge at the same value of χ is shown by the red line. On this line a dramatic change of the length scale occurs: the dominant fluctuations destroying the spatially uniform disordered state have considerably longer wave length above the line than below it.

Now, let us compare the phase behavior of the $A_{fmN}(B_{N/2}A_{N/2})_nB_{(1-f)mN}$ copolymers in the whole (n,m)

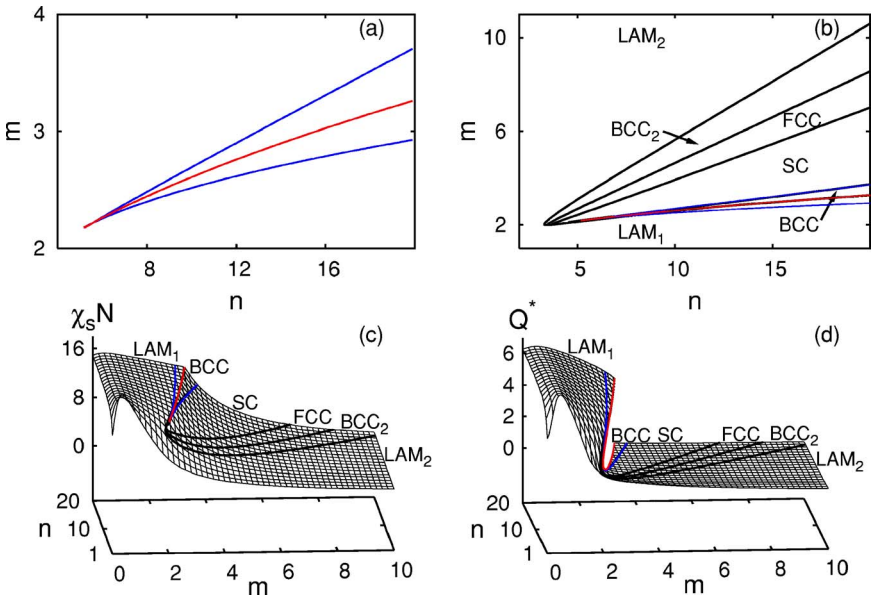

FIG. 2. (a) Classification diagram for the symmetric system $A_{mN/2}(B_{N/2}A_{N/2})_nB_{mN/2}$. Blue lines delineate the bifurcation region. Red line inside the bifurcation region is the equimaxima line, where a dramatic change of length scales occurs. (b) Phase diagram in the (n,m) plane. Solid lines show the phase-transition lines, the blue lines depict the bifurcation region. (c) Spinodal χ_sN values. (d) Characteristic dimensionless inverse length scale $Q^*=(q^*R_g(N))^2$, where $R_g(N)$ is the radius of gyration of the repeat unit (AB diblock).

plane and that of the particular case of diblock copolymers $A_{fN}B_{(1-f)N}$. For the latter the ODT is typically a discrete first-order phase transition and it is a continuous second-order phase transition (within the mean-field approximation of the WST) in the only critical point $f=0.5$, where the coefficient α of the third-order term in the expansion of free energy (8) vanishes due to the copolymer symmetry. Similarly, the ODT is a second-order phase transition for the symmetric $A_{mN/2}(B_{N/2}A_{N/2})_nB_{mN/2}$ copolymers for any physical value of $m\geqslant 0$ and integer $n>0$. Indeed, the state of the symmetric systems is not changed after interchange of A and B monomers and, therefore, the free energy (2) should remain unchanged after replacing Ψ_A by $\Psi_B=-\Psi_A$, which is only possible if all the terms of the free energy with odd powers of the order parameter vanish. Vanishing of the cubic term can, of course, be checked also via straightforward calculation.

All the critical points are located on the spinodal surface in the space (n,m,χ_s). The ODT in the critical point is the DIS-LAM transition for the case of diblock copolymers, but for the symmetric $A_{mN/2}(B_{N/2}A_{N/2})_nB_{mN/2}$ multiblock copolymers the ordered phase arising in the critical point can have the symmetry of the LAM, BCC, SC, FCC, or BCC_2 phases depending on the values of the structural parameters n,m. The resulting phase diagram for the symmetric copolymers can be calculated straightforwardly[46] and its projection on the (n,m) plane is shown in Fig. 2(b). One can see from Fig. 2(b), that there are different sequences of the order-disorder transitions upon increasing m along a line crossing the bifurcation region for fixed n. For $n\leqslant 3$ the only ordered phase below the critical temperature is the lamellar one, its periodicity being strongly m dependent. With the increase of the relative length of the tails m the sequences LAM_1-SC -FCC-BCC_2-LAM_2 and LAM_1-BCC-SC-FCC- BCC_2-LAM_2 of stable morphologies occur for $n=4$ and $n\geqslant 5$, respectively, the periodicity of LAM_1 being much smaller than that of LAM_2 (see Figs. 2(d) and 8 further on). The existence of two lamellar morphologies with rather different periodicity illustrates the presence and interplay of two competing length scales in the system. The phase-transition lines BCC-SC and LAM_1-BCC are so close to the upper boundary of the bifurcation region and the equimaxima line, respectively, that the corresponding lines merge on the scale of Fig. 2(b).

To understand the validity of the presented phase diagram it is worth noting that the equilibrium free energy has been calculated by taking into account the dominant maximum only. Considering also that the WST is applicable close to the critical points, we conclude that this approximation is, obviously, valid outside the bifurcation region but is questionable close to the equimaxima line, where both maxima are important [see Fig. 2(a)]. Thus, all the phase-transition lines but LAM_1-BCC can be considered as well validated.

The values of the χ parameter corresponding to the order-disorder transitions as well as the reduced critical wave length $Q^*=(q^*R_g(N))^2$ are shown in Figs. 2(c) and 2(d), respectively, as functions of m and n. The bifurcation region border and equimaxima line are depicted with the blue and red lines, respectively. For $m=0$ the system corresponds to a symmetric multiblock copolymer melt. It demonstrates the standard asymptotic behavior of Q^* and χ_sN with increasing n.[33,34,47,48] For larger m the system behaves like a symmetric ABC triblock melt with a nonselective middle block B[25,29,30] (due to the structure symmetry the effective interactions between the middle multiblock part and two tail blocks are the same). Asymptotically, with increasing value of m both surfaces of Fig. 2 approach the zero-level plane, which is quite natural. Indeed, the number of monomers involved in ordering on the short length scale is N, whereas that for the ordering on the long length scale is $N_{\mathrm{tot}}=N(n+m)$. The transition temperatures for the first and the second case are χ_sN and $\chi_sN(n+m)$, respectively. Hence, with increasing m the ODT of the long length scale occurs at $\chi_sN=\mathrm{const}/(n+m)$.

B. Asymmetric systems

Now we proceed to the general case of molten block copolymers $A_{fmN}(B_{N/2}A_{N/2})_nB_{(1-f)mN}$ with $f\neq 0.5$, which enables us to study the tail (homopolymer end block) asymmetry influence on the phase diagrams. Obviously, due to the

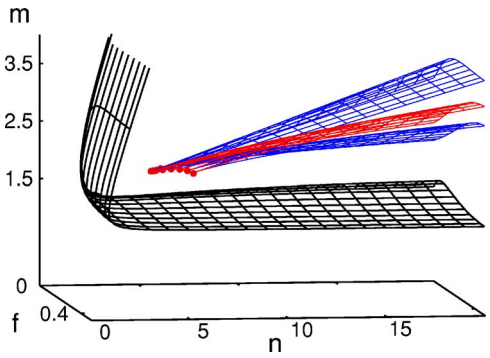

FIG. 3. The characteristic surfaces in the (n,f,m) space for asymmetric $A_{fmN}(B_{N/2}A_{N/2})_nB_{(1-f)mN}$ multiblock copolymers. The black, blue, and red wire surfaces are the critical, bifurcation, and equimaxima surfaces, respectively. The red solid line with dots shows variation of the bifurcation point as the parameter f varies from 0.5 to 0.

macromolecule symmetry the interval $0 \leqslant f \leqslant 0.5$ is only of interest. To remain within the range of validity of the WST we need to be close to the critical point and, therefore, we start with plotting the classification and critical surfaces in the (n,f,m) space (see Fig. 3). By fixing $f \in [0,0.5)$ and solving Eq. (28) we obtain a line of critical points in the (n,m) plane. The upper (lower) branch of the line corresponds to the larger (smaller) values of m and describes the critical points for the long (short) length scale region. As explained above, when $f \to 0.5$ the absolute value of the cubic coefficient α approaches zero for all values of parameters n and m and, therefore, the critical points surface in this case is the whole plane (n,m).

We plot phase diagrams for asymmetric systems in the $(f,\chi N)$ plane in the vicinity of the critical point $f=0.5$ and outside the bifurcation region (see Fig. 4). To discuss the phase behavior of asymmetric systems we fix two sets: $n=3$ and $n=10$. Phase diagrams for the set $n=3$ are plotted in Fig. 5. The main observation here is that there is an interval

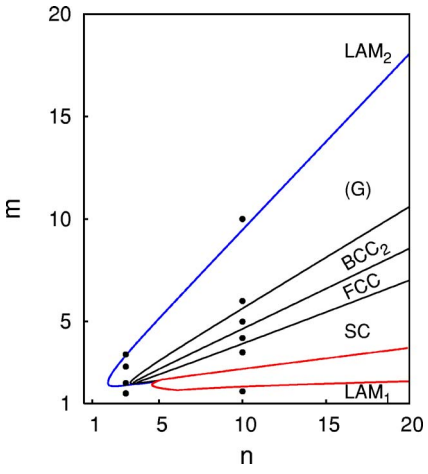

FIG. 4. The legend for the phase diagrams of the symmetric $A_{mN/2}(B_{N/2}A_{N/2})_nB_{mN/2}$ multiblock copolymers. The dots correspond to the values of the structural parameters n and m, for which the phase diagrams in the $(f,\chi N)$ plane are presented on the subsequent figures. Solid lines indicate the ODT phase diagram for the symmetric systems. Red solid line delineates the projection of the bifurcation region into (n,m) plane. The blue and top red lines demarcate the region where the gyroid (G) phase is stable for some value of $f \in (0,0.5)$.

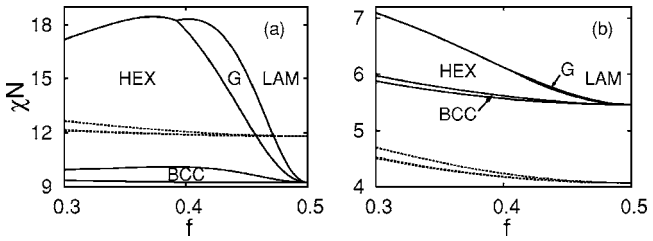

FIG. 5. Phase diagrams in the $(f,\chi N)$ plane for asymmetric systems with $n=3$ and various tail block lengths: (a) $m=1.5$ and $m=2$ (dashed and solid lines, respectively); (b) $m=2.8$ and 3.4 (solid and dashed lines, respectively). Phase diagrams depicted with dashed lines have only conventional phases. The BCC and HEX phase lines in these diagrams are very close to each other due to the scale used.

of values of m where G phase is stable in the vicinity of the critical point. This region of the G phase stability in the whole plain (n,m) is depicted with blue and top red lines in Fig. 4. When the number of diblock units in the middle part is not large, the length scale of microphase separation changes gradually upon varying the length of the tail blocks. For large values of n the phase behavior changes. The values of the parameter m for the set $n=10$ are chosen in such a way that for the corresponding symmetric system there exist different stable phases.

Upon changing the relative length of the tail blocks m for $n=10$ the system demonstrates a considerably larger set of characteristic phase diagrams shown in Figs. 6 and 7. In this case the equimaxima line in the bifurcation region is crossed when changing the parameter m (see Figs. 2 and 4), which results in an abrupt change of the phase diagram topology. We start with $m=1.6$, where the stable phases are the conventional ones [BCC, HEX, and LAM_1, see Fig. 6(a)], which is quite understandable. Indeed, if the total length of the tail blocks is not large as compared to the length of the middle multiblock part, then the short length scale ordering only should occur in the system under consideration and its phase diagram should resemble that of periodic multiblock copolymer melts.[10] Upon increasing the total length of the tail blocks, the system starts to behave like the linear ABC block copolymer with a long nonselective middle block. Accordingly, microphase separation occurs at the large length scale.

For the systems with values of m just slightly above the bifurcation region large values of χN are required for the BCC_2 and FCC structures to be stable. Therefore, the WST predictions are hardly valid for these phases. We plot phase diagrams for larger values of m, which are far beyond the bifurcation region, and various nonconventional cubic symmetry structures appear within the region of the WST validity [see Figs. 6(b) and 7]. Several examples are presented in Fig. 7. Figure 7(d) corresponds to $m=10$, where the middle multiblock has the same length as both tail blocks together. The phase diagram for this composition belongs to the same universality class as that for diblock copolymer. The border of the BCC phase in the latter system is very close to the border of the HEX phase on the scale used.

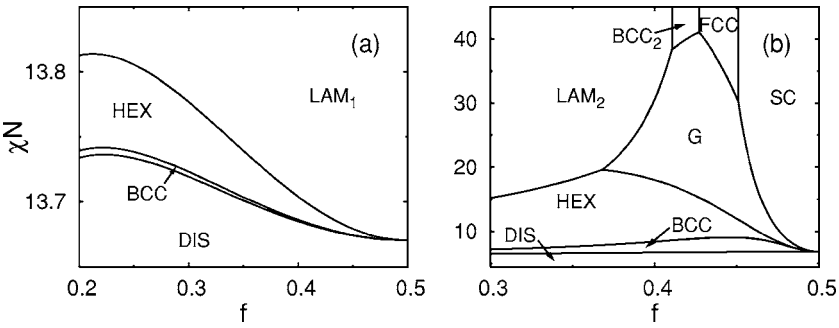

FIG. 6. Phase diagrams in the $(f,\chi N)$ plane for asymmetric systems with $n=10$ and $m=1.6$ (a) and $m=3.5$ (b). Regions of stability of different phases are labeled with corresponding letters.

The asymmetry dependence of the reduced squared wave numbers corresponding to the six phase diagrams above with increasing parameter m is shown in Fig. 8. The upper line corresponds to $m=1.6$, i.e., below the bifurcation region, whereas the next line corresponds to $m=3.5$, i.e., above the bifurcation region. The plot clearly shows the dramatic change in length scale when the parameters of the system cross the bifurcation region. The phase behavior for larger values of n is qualitatively similar to that for $n=10$.

IV. CONCLUSION

It is shown that the predictions of the classical weak segregation theory of microphase separation as applied to some specially designed binary AB block copolymers are not limited to the conventional phases of lamellar, hexagonal, and body-centered structures. As exemplified by the results presented in the preceding section, the phase behavior of $A_{fmN}(B_{N/2}A_{N/2})_nB_{(1-f)mN}$ block copolymers is much richer than that of simple diblock copolymers,[1,16] even in the first harmonic approximation of the weak segregation regime. If the number n of elementary diblock units forming the middle multiblock part of the macromolecules exceeds 2, there is a region in the (n,m,f) space where the (double) gyroid phase stays stable in a certain temperature interval up to the very critical point $f=0.5$. For $n>3$ there are regions in the (n,m) plane, where the nonconventional cubic phases FCC, SC, or the noncentrosymmetric cubic phase BCC_2 (Ref. 20) (single gyroid) replace the LAM phase as the most stable low-temperature phase. For $n>5$ a continuous change of m results in an abrupt jump not only in the symmetry but also in the periodicity of the ordered phases (for $n=10$ up to ten times as shown in Fig. 8), which is the most transparent manifestation of the two-length-scale nature of the system. Even though the SCFT is known to describe well the order-order transitions accompanied by such changes in periodicity (see Refs. 28 and 49, where the change in periodicity was up to three times), we believe that our WST analysis would provide valuable guidance to any future SCFT calculation. Another important and still open issue is which new morphologies can appear in the vicinity of the equimaxima line in the bifurcation region, where the contributions of the Fourier components of the order parameter with two different wave lengths are comparable. The two problems may interplay when modifying the SCFT to study the evolution of the structures occurring in the symmetric system $(f=0.5)$ at the ODT with decreasing temperature until microphase separation occurs on both length scales.

To conclude, we believe that the phenomenon of the two-length-scale switching between the different ordered morphologies reported in Refs. 23, 24, and 28 as well as in

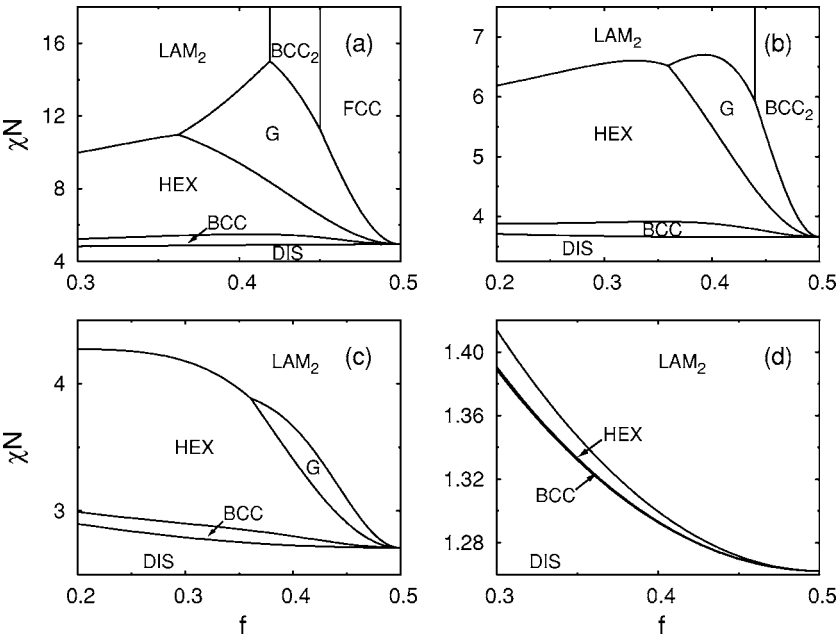

FIG. 7. Phase diagrams in the $(f,\chi N)$ plane for asymmetric systems with $n=10$ and $m=4.2$ (a), $m=5$ (b), $m=6$ (c), and $m=10$ (d).

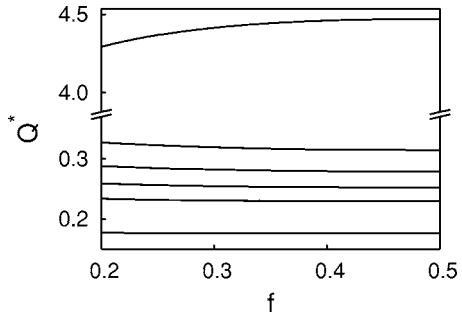

FIG. 8. Plot of the dimensionless inverse length scale of microphase separation vs the asymmetry parameter for the set $n=10$. From top to bottom: $m=1.6, 3.5, 4.2, 5, 6$, and 10. Here $Q^*=(q^*R_g(N))^2$ and the corresponding length scales can be found from $L/R_g(N)=2\pi/\sqrt{Q^*}$.

the present paper is to be expected in various copolymer systems characterized by a two-scale compositional inhomogeneity.

ACKNOWLEDGMENTS

The work was supported by NWO and RFBR (Grant No. NWOa 04-03-89002). We also acknowledge useful discussions with R. J. Nap.

APPENDIX: THE SECOND STRUCTURAL CORRELATORS

The second structural correlators appearing in Eq. (4) read

$$g_{AA}(x)=\frac{2}{N_{\mathrm{tot}}}[nF_D(x,0.5)+F_D(x,mf)+\exp(-xN/2)p(x,0.5)[p(x,0.5)S_2(x,n)+p(x,mf)S_1(x,n)]],$$

$$g_{AB}(x)=\frac{1}{N_{\mathrm{tot}}}[p(x,0.5)S_1(x,n)[p(x,mf)+p(x,m(1-f))]+p(x,mf)p(x,m(1-f))\exp(-xnN)+p^2(x,0.5)\times[S_2(x,n)+S_2(x,n+1)]].$$

Here $x=(aq)^2/6$ and we introduce the auxiliary functions,

$$p(x,f)=[1-\exp(-xfN)]/x,$$

$$F_D(x,f)=[\exp(-xfN)-1+xfN]/x^2,$$

$$S_1(x,n)=[1-\exp(-xnN)]/[1-\exp(-xN)],$$

$$S_2(x,n)=[\exp(-xnN)-n\exp(-xN)+n-1]/[1-\exp(-xN)]^2.$$

The correlation function $g_{BB}(x)$ can be obtained from the expression for $g_{AA}(x)$ if one substitutes $(1-f)$ instead of f.

[1] L. Leibler, Macromolecules **13**, 1602 (1980).
[2] F. Bates and G. Fredrickson, Annu. Rev. Phys. Chem. **41**, 525 (1990).
[3] I. Erukhimovich and A. Khokhlov, Polymer Science Series A 35, 1808 (1993).
[4] K. Binder, Adv. Polym. Sci. **112**, 181 (1994).
[5] P. de Gennes, Faraday Discuss. Chem. Soc. **68**, 96 (1979).
[6] I. Erukhimovich, Polymer Science Series A 24, 2223 (1982).
[7] F. Bates and G. Fredrickson, Phys. Today **52**2, 32 (1999).
[8] G. Fredrickson and E. Helfand, J. Chem. Phys. **87**, 697 (1987).
[9] A. Mayes and M. O. de la Cruz, J. Chem. Phys. **91**, 7228 (1989).
[10] A. Dobrynin and I. Erukhimovich, Macromolecules **26**, 276 (1993).
[11] L. Landau, Phys. Zs. Sowjet. **11**, 26 (1937).
[12] S. Alexander and J. McTague, Phys. Rev. Lett. **11**, 702 (1978).
[13] J. Toledano and P. Toledano, *The Landau Theory of Phase Transitions* (World Scientific, Singapore, 1987).
[14] E. Kats, V. Lebedev, and A. Muratov, Phys. Rep. **228**, 1 (1993).
[15] J. Huh and W. Jo, Macromolecules **37**, 3037 (2004).
[16] M. Matsen and M. Schick, Phys. Rev. Lett. **72**, 2660 (1994).
[17] M. Matsen and F. Bates, Macromolecules **29**, 1091 (1996).
[18] D. Hajduk, P. Harper, S. Gruner, C. Honeker, G. Kim, E. Thomas, and L. Fetters, Macromolecules **27**, 4063 (1994).
[19] S. Förster, A. Khandpur, J. Zhao, F. Bates, I. Hamley, A. Ryan, and W. Bras, Macromolecules **27**, 6922 (1994).
[20] S. Brazovskii, I. Dzyaloshinski, and A. Muratov, Sov. Phys. JETP **66**, 625 (1987).
[21] I. Erukhimovich, JETP Lett. **63**, 459 (1996).
[22] R. Hołyst and M. Schick, J. Chem. Phys. **96**, 7728 (1992).
[23] R. Nap, C. Kok, G. ten Brinke, and S. Kuchanov, Eur. Phys. J. E **4**, 515 (2001).
[24] R. Nap and G. ten Brinke, Macromolecules **35**, 952 (2002).
[25] I. Erukhimovich, in *Proceedings of the International Conference on Advance Polymers and Processing ICAPP*, Yonezawa, Japan, edited by K. Iwakura (ICAPP, Yonezawa, 2001), pp. 122–128.
[26] I. Erukhimovich, Y. Smirnova, and V. Abetz, Polymer Science Series A 45, 1093 (2003).
[27] S. Tarasenko and I. Erukhimovich, Polymer Science Series A 47, 229 (2005).
[28] R. Nap, I. Erukhimovich, and G. ten Brinke, Macromolecules **37**, 4296 (2004).
[29] I. Erukhimovich, cond-mat/0405569.
[30] I. Erukhimovich, Eur. Phys. J. E **18**, 383 (2005).
[31] I. Erukhimovich and A. Dobrynin, Macromol. Symp. **81**, 253 (1994).
[32] S. Panyukov and I. Potemkin, JETP **85**, 183 (1997).
[33] I. Erukhimovich, Polymer Science Series A 24, 2232 (1982).
[34] H. Benoit and G. Hadziioannou, Macromolecules **21**, 1449 (1988).
[35] T. Kavassalis and M. Whitmore, Macromolecules **24**, 5340 (1991).
[36] M. Matsen and M. Schick, Macromolecules **27**, 7157 (1994).
[37] P. Flory, *Principles of Polymer Chemistry* (Cornell University Press, Ithaca, New York, 1953).
[38] E. Shakhnovich and A. Gutin, J. Phys. (France) **50**, 1843 (1989).
[39] S. Panyukov and S. Kuchanov, J. Phys. II France 2, 1973 (1992).
[40] G. Fredrickson, S. Milner, and L. Leibler, Macromolecules **25**, 6341 (1992).
[41] H. Angerman, G. ten Brinke, and I. Erukhimovich, Macromolecules **29**, 3255 (1996).
[42] H. Angerman, G. ten Brinke, and I. Erukhimovich, Macromolecules **31**, 1958 (1998).
[43] U. Shmueli, *International Tables for Crystallography* (Kluwer Academic, Dortdrecht, 1996), Vol. B.
[44] M. Wohlgemuth, N. Yufa, J. Hoffman, and E. Thomas, Macromolecules **34**, 6083 (2001).
[45] S. Milner and P. Olmsted, J. Phys. II France 7, 249 (1997).
[46] Y. Smirnova, G. ten Brinke, and I. Erukhimovich, Polymer Science Series A 47, 430 (2005).
[47] Y. Matsushita, Y. Mukai, H. Mogi, J. Watanabe, and I. Noda, Polymer **35**, 246 (1994).
[48] R. Spontak and S. Smith, J. Polym. Sci., Part B: Polym. Phys. **39**, 947 (2001).
[49] M. Matsen, J. Chem. Phys. **103**, 3268 (1995).